Time-resolved dynamics in iodide-uracil-water clusters upon excitation of the nucleobase

Alice Kunin[1], Valerie S. McGraw[1], Katharine G. Lunny[1], and Daniel M. Neumark[1,2,a)]

[1]*Department of Chemistry, University of California, Berkeley, California 94720, USA.*
[2]*Chemical Sciences Division, Lawrence Berkeley National Laboratory, Berkeley, California 94720, USA.*

[a)]Author to whom correspondence should be addressed. E-mail: dneumark@berkeley.edu.

Abstract

The dynamics of iodide-uracil-water ($I^-\cdot U\cdot H_2O$) clusters following π-π^* excitation of the nucleobase are probed using time-resolved photoelectron spectroscopy (TRPES). Photoexcitation of this cluster at 4.77 eV results in electron transfer from the iodide moiety to the uracil, creating a valence-bound (VB) anion within the cross-correlation of the pump and probe laser pulses. This species can decay by a number of channels, including autodetachment and dissociation to I^- or larger anion fragments. Comparison of the energetics of the photoexcited cluster and its decay dynamics with those of the bare iodide-uracil ($I^-\cdot U$) complex provide a sensitive probe of the effects of microhydration on these species.

I. INTRODUCTION

DNA damage has been shown to proceed directly from UV photoexcitation, as well as indirectly from the attachment of low-energy electrons to its constituent nucleobases.[1-4] DNA bases exhibit strong absorption cross-sections for UV radiation, particularly near 260 nm (4.77 eV),[5, 6] and the interaction of nucleobases with surrounding solvent water molecules plays a key role in the relaxation and photostability of nucleobases in this excitation energy regime.[7, 8] The attachment of low-energy electrons induces strand breaks in DNA,[2-4] and it has been proposed that the initial site of electron attachment is the nucleobase followed by electronic coupling that facilitates fragmentation at the backbone.[9-16] Photoelectron spectroscopy has shown that the addition of water increases the electron affinity of nucleobases,[17, 18] while molecular dynamics simulations find that solution-structure fluctuation likely promotes attachment of bulk hydrated electrons to nucleobases.[19] Our group has previously examined the ultrafast dynamics of electron attachment to nucleobases using time-resolved photoelectron spectroscopy[20] (TRPES) of various iodide-nucleobase ($I^-\cdot N$) complexes[21-27] and related model systems.[28, 29] The present study uses TRPES to examine iodide-uracil-water ($I^-\cdot U\cdot H_2O$) clusters photoexcited at 260 nm and compares these results to those of iodide-uracil ($I^-\cdot U$) to understand the role of water in the mechanisms of excitation and charge transfer in these anionic clusters in this UV excitation regime.

$I^-\cdot N$ complexes have been previously studied by photofragment action spectroscopy[26, 30, 31] and electronic structure calculations[26, 30, 32] in addition to TRPES. Two regimes of UV photoabsorption have been measured for these complexes.[26, 30, 31] The first is centered near the vertical detachment energy (VDE), the difference in energy between the anion and the neutral

clusters at the equilibrium geometry of the anion, which is approximately 4 eV for most $I^-\cdot N$ clusters.[21, 22, 25] The second region of UV photoabsorption is a broad band spanning ~4.6 – 5.0 eV. Excited state calculations for $I^-\cdot U$,[26] iodide-thymine ($I^-\cdot T$),[30] and $I^-\cdot U\cdot H_2O$[32] show that photoexcitation near the VDE corresponds to optical excitation from the iodide (5p) orbital to a dipole-bound (DB) state of the nucleobase. The nucleobase DB state arises from capture of the excess electron by the relatively large dipole moment of the base.[33-37] In contrast, these same calculations indicate that photoexcitation near 4.7 – 4.8 eV primarily corresponds to base-centered π-π* excitation. The dynamics resulting from near-VDE photoexcitation of $I^-\cdot U\cdot H_2O$ and the effects therein of the water molecule have already been considered in detail,[32] so we focus here only on the effect of the addition of water on the dynamics ensuing π-π* photoexcitation.

TRPES of $I^-\cdot N$ clusters probes the dynamics of photoinduced electron attachment and electronic excitation in nucleobases and traces the time evolution of nascent transient negative ions (TNIs) and anionic decay photofragments. Our TRPES studies with pump excitation energies from 4.60 – 4.90 eV are expected to create a π-π* excited state of the nucleobase, as in Eq. 1:

$$I^-(5p^6)\cdot N(\pi^4\pi^{*0}) \xrightarrow{h\nu_{pump}\ \sim 260\ nm} I^-(5p^6)\cdot N(\pi^3\pi^{*1}) \qquad (1)$$

Time-resolved studies in this pump excitation regime have found instantaneous formation of the cluster valence-bound (VB) anion with no evidence for the presence of DB states.[21, 22] The VB state corresponds to electron attachment to a valence orbital, the π* orbital of the base.[14, 17, 38]

We have previously proposed[21, 27] for $I^-\cdot U$ and $I^-\cdot T$ complexes that, subsequent to π-π* excitation of the nucleobase, charge transfer from iodide to the empty π orbital creates the VB anion. While this overall mechanism is consistent with experimental results and electronic structure calculations,[27] it still awaits theoretical confirmation.

Photofragment action spectroscopy in conjunction with TRPES has identified autodetachment as well as formation of I^- as the major cluster decay pathways in both photoexcitation regimes for $I^-\cdot U$ binary clusters,[26] although the nature of the time-resolved dynamics of these channels has been found to be clearly different for each set of pump energies.[27] Autodetachment refers to the spontaneous emission of an electron from photoexcitation of an anion resonance embedded within the neutral plus free electron continuum;[39-41] these electrons can be very slow if randomization of vibrational energy occurs prior to electron emission (the thermionic emission limit).[42]

In the present study, we employ TRPES to excite $I^-\cdot U\cdot H_2O$ complexes near the peak of the base-centered π-π* excitation[32] at 260 nm (4.77 eV), and track the resulting dynamics with 1.58 eV or 3.18 eV probe pulses. These experiments, which complement previous work[32] on near-VDE excitation of $I^-\cdot U\cdot H_2O$ complexes, probe the dynamics of both electronically excited uracil as well as the interaction of low-energy electrons with the nucleobase. TRPES can identify and trace the dynamics of nascent TNIs (eBE ~ 0 eV – 1 eV)[18, 34, 38, 43-46] with 1.58 eV probe pulses, while the higher energy probe is capable of detecting anionic photofragments such as I^- (neutral electron affinity = 3.059 eV).[47] Here, we observe prompt formation of the VB anion, with autodetachment and the formation of I^- as the major decay channels for the photoexcited clusters. The lifetimes of the VB anion and autodetachment features reflect the stabilizing effect

of the presence of water, while the I^- rise dynamics suggest that additional water-associated fragmentation channels may be active here.

II. EXPERIMENTAL METHODS

The experimental apparatus employed in this study has been described in detail previously[48, 49] and is briefly summarized here. $I^-\cdot U\cdot H_2O$ clusters were generated by passing 515 kPa helium buffer gas over a reservoir of distilled water and a reservoir of methyl iodide (CH_3I). The reservoirs and the connecting gas line were wrapped in heating tape; the water reservoir was heated to approximately 30 °C, while the CH_3I reservoir and gas line were heated to approximately 40 °C. The gas mixture was then passed through an Even-Lavie pulsed valve operating at 500 Hz, which contained a sample cartridge of uracil (Sigma-Aldrich, ≥99%) heated to 240 °C. The gas mixture was expanded into vacuum through a ring-filament ionizer to create anionic clusters, which were then extracted orthogonally into a Wiley-McLaren time-of-flight mass spectrometer.[50] The $I^-\cdot U\cdot H_2O$ clusters were mass-selected and then intersected by the pump and probe laser pulses.

To generate the pump and probe laser pulses, a KMLabs Griffin Oscillator and Dragon Amplifier were used to produce 45 fs pulses centered at approximately 785 nm (1.58 eV) with 1.8 mJ/pulse. The fundamental was frequency tripled with two β-barium borate (BBO) crystals to produce ~10 μJ/pulse of 260 nm (4.77 eV) pump pulses. The residual 785 nm pulses were recovered from the frequency-tripler set-up, and were sent to a delay stage to serve as probe pulses of ~80 μJ/pulse. Alternatively, this recovered 785 nm light was frequency-doubled in a BBO to produce ~60 μJ/pulse of 390 nm (3.18 eV) probe pulses. In either case, the pump and probe pulses were combined at the chamber in a dichroic beamsplitter. The cross-correlation of

260 nm/785 nm was ≤180 fs and that of 260 nm/390 nm was <300 fs; the latter cross-correlation, measured outside the chamber, is obscured by residual 390 nm light, and the actual cross-correlation is expected to be as much as 50-100 fs shorter than this measured value.[26]

The resultant photoelectrons were analyzed by a velocity-map imaging assembly[51] comprising three electron optical elements and a chevron-stacked microchannel plate detector coupled to a phosphor screen imaged by a charge-coupled device camera. Basis-set expansion (BASEX) reconstruction methods were used to reconstruct the 3D photoelectron kinetic energy (eKE) distributions.[52]

III. RESULTS

Fig. 1 presents a laser noise-subtracted, single-photon photoelectron spectrum of $I^-\cdot U\cdot H_2O$ clusters photodetached at 4.74 eV, as well as an image of the calculated ground state structure of the cluster.[32] The photoelectron spectrum is provided as a function of eKE as well as electron binding energy (eBE) (eBE = $h\nu_{photon}$ – eKE). Two features appear in this spectrum: feature A, peaked at approximately 4.69 ± 0.05 eV eBE (0.05 ± 0.05 eV eKE), and feature B, peaked at 4.40 ± 0.05 eV eBE (0.37 ± 0.05 eV eKE). As has been previously determined,[32] feature A corresponds to autodetachment of ~0 eV eKE electrons from the photoexcited $I^-\cdot U\cdot H_2O$ clusters, and feature B corresponds to direct detachment to the lower iodine spin-orbit state ($^2P_{3/2}$) from the $I^-\cdot U\cdot H_2O$ anion, yielding a VDE of 4.40 eV for $I^-\cdot U\cdot H_2O$. As both of these features arise from single-photon (pump-only) processes at the pump energy employed in our TRPES experiments, they are also present in all of the TRPE spectra here at these same eKEs.

Fig. 2 presents photoelectron spectra at select time delays for $I^-\cdot U\cdot H_2O$ at 4.77 eV pump excitation energy and 1.58 eV probe energy; here and in other TRPE spectra, eBE = $h\nu_{probe}$ –

eKE. Feature A exhibits non-zero intensity at negative times and increases in intensity over approximately 10 ps before decreasing back to its initial intensity. Feature B exhibits noisy but similar time dynamics as feature A, likely due to spectral overlap between the two features in this region. Feature C, covering the region from approximately 0.1 eV – 0.9 eV eBE, is enlarged in the inset. Based on our previous results on $I^-\cdot U$ clusters photoexcited at excitation energies in the range of 4.69 – 4.90 eV,[21, 22] we can assign feature C as the VB anion of photoexcited $I^-\cdot U\cdot H_2O$. Time-resolved photoelectron spectra for feature C, background-subtracted with respect to the most negative delay time, are shown in Fig. 3 for time delays up to 5 ps.

Fig. 4 presents photoelectron spectra at select time delays for $I^-\cdot U\cdot H_2O$ at 4.77 eV pump excitation energy and 3.18 eV probe energy. Features A and B are the same features seen in Fig. 2. The prominent new feature in these spectra, feature D, is located at 3.06 ± 0.05 eV eBE, and this narrow feature grows monotonically in intensity over the course of experiment. Based on the binding energy, spectral shape, and time-dynamics of feature D, we assign feature D to photodetachment of atomic iodide to the $^2P_{3/2}$ iodine spin-orbit state. Background-subtracted time-resolved photoelectron spectra for features A and D are presented in Fig. 5.

IV. ANALYSIS

The normalized, integrated intensities for the VB anion (red, feature C) and the autodetachment feature (black, feature A) are shown at early, intermediate, and long time delays in Fig. 5. The integrated signals are fit to the convolution of a Gaussian instrumental response function with *i* exponential functions as in Eq. 2:

$$I(t) = \frac{1}{\sigma_{CC}\sqrt{2\pi}} \exp\left(\frac{-t^2}{2\sigma_{CC}^2}\right) \cdot \begin{cases} I_0, t < 0 \\ I_0 + \sum_i A_i \exp\left(\frac{-t}{\tau_i}\right), t \geq 0 \end{cases} \quad (2)$$

In this equation, σ_{cc} is the Gaussian full width at the half-maximum given by the cross-correlation of the pump and probe laser pulses, I_0 is the signal background, A_i are the coefficients for each exponential function, and τ_i are the corresponding rise or decay lifetimes for each exponential. These fits are shown in Fig. 5 as solid red and black lines for the VB anion and autodetachment features, respectively. The VB anion is found to appear within the cross-correlation of the pump and probe laser pulses and decay bi-exponentially. The fits for the $I^-\cdot U\cdot H_2O$ VB anion decay are 540 ± 240 fs and 220 ± 70 ps. The autodetachment feature was found to remain relatively constant in intensity at negative times. At positive delay times this feature rises to a maximum in 11.3 ± 2.2 ps followed by decay to the negative-time intensity in approximately 285 ± 70 ps.

For ease of comparison to our previous work on $I^-\cdot U$ clusters, the normalized, integrated intensities for the VB anion and autodetachment produced from $I^-\cdot U$ photoexcited at 4.79 eV are presented in Fig. 7 in purple, overlaid with the corresponding $I^-\cdot U\cdot H_2O$ features (green) from Fig. 5. Fig. 8 presents the normalized integrated intensity and fitted rise for the I^- signal observed here. The I^- formation was found to be bi-exponential, with rise time constants of 32.5 ± 2.6 ps and 230 ± 20 ps. Table I summarizes the fit rise and decay lifetimes for the VB anion, autodetachment, and I^- feature for $I^-\cdot U\cdot H_2O$ in the present study and for $I^-\cdot U$ photoexcited at 4.79 eV from our past work.[21, 26]

V. DISCUSSION

This work explores the dynamics of $I^-\cdot U\cdot H_2O$ clusters photoexcited at 4.77 eV, resonant with the base-centered π-π* transition for uracil. We observe instantaneous formation of the VB anion of the cluster following photoexcitation, and bi-exponential decay of this species with time constants of 540 fs and 220 ps. Autodetachment and I^- re-formation are observed as decay channels in this photoexcitation regime. These experiments show that to first order, the dynamics of photoexcited $I^-\cdot U\cdot H_2O$ are similar to those of $I^-\cdot U$ following π-π* photoexcitation. However, the addition of a water molecule noticeably affects the rise time of the I^- signal as well as the decay dynamics of the VB state, as can be seen from Fig. 6 and Table I. As summarized in Eq. 3 below, we have previously proposed that the initial π-π* iodide-associated photoexcited state decays by two pathways: the π-π* excited nucleobase state internally converts to the ground state of the cluster and subsequently evaporates iodide, or iodide transfers a valence electron to fill the hole in the nucleobase π orbital, creating a VB anion that then decays by autodetachment.[27]

$$\begin{aligned} I^-(5p^6)\cdot N(\pi^4\pi^{*0}) &\xrightarrow{h\nu_{pump}\ \sim 260\ nm} I^-(5p^6)\cdot N(\pi^3\pi^{*1}) \\ I^-\cdot N(\pi^3\pi^{*1}) &\xrightarrow[\text{Conversion}]{\text{Internal}} I^-\cdot N \rightarrow I^- + N \\ &\rightarrow I\cdot N^-(\pi^4\pi^{*1}) \xrightarrow{\text{Autodetachment}} I\cdot N + e^- \end{aligned} \tag{3}$$

TRPES on $I^-\cdot U\cdot H_2O$ at this pump energy is sensitive to each of these decay channels. In the subsections that follow, we consider the iodide formation, VB anion, and autodetachment dynamics and the effect of the added water to expand on the basic framework previously set forward.

A. Iodide formation dynamics

TRPES of π-π* photoexcited $I^-\cdot U\cdot H_2O$ clusters finds bi-exponential I^- formation in 32.5 ps and 230 ps, in contrast to $I^-\cdot U$ clusters for which I^- was found to appear mono-exponentially in 36 ps.[26] As in Eq. 3, we have suggested that due to the previously observed strong connection between the VB anion and the autodetachment dynamics in this pump energy regime, the base-centered π-π* excitation is followed by internal conversion to the ground state and subsequent dissociation to produce iodide mono-exponentially.[27] While this mechanism is likely the source of the fast I^- rise signal, it alone cannot fully explain the origin of the bi-exponential I^- appearance observed here for $I^-\cdot U\cdot H_2O$ clusters.

Several energetically accessible dissociation channels have been previously calculated for $I^-\cdot U\cdot H_2O$ clusters, including dissociation to yield $I^-\cdot H_2O$ clusters.[32] $I^-\cdot H_2O$ produced as a dissociation product upon photoexcitation could also then further dissociate to yield a second source of I^- signal with a delayed rise time, contributing to the bi-exponential rise dynamics observed here, as depicted in Eq. 4:

$$\begin{aligned} I^-\cdot U\cdot H_2O &\xrightarrow{h\nu_{pump}\ \sim 260\ nm} I^-\cdot U(\pi^3\pi^{*1})\cdot H_2O \\ I^-\cdot U(\pi^3\pi^{*1})\cdot H_2O &\xrightarrow{\text{Internal Conversion}} I^-\cdot U\cdot H_2O \rightarrow I^- + U\cdot H_2O \\ &\rightarrow I^-\cdot H_2O + U \rightarrow I^- + H_2O + U \end{aligned} \qquad (4)$$

TRPES experiments of $I^-\cdot U\cdot H_2O$ clusters photoexcited at 4.77 eV pump energy and probed by 4.0 eV and by 4.77 eV probe energies were unable to conclusively identify the formation of $I^-\cdot H_2O$ (VDE = 3.51 ± 0.02 eV)[53, 54] due to poor overall signal levels at these probe energies. However, the existence of this dissociation channel could be verified in future experiments by photofragment action spectroscopy, for example.

B. VB anion formation and decay dynamics

As seen in Fig. 3, the VB anion of $I^-\cdot U\cdot H_2O$ exhibits the strongest intensity near eBE = 0.8 – 0.9 eV, which is approximately 0.2 – 0.3 eV higher than the strongest intensity for the $I^-\cdot U$ VB anion from our past work in this π-π* pump excitation energy regime.[21, 22] This finding indicates that the presence of water stabilizes the VB anion. In our past work on near-VDE photoexcited $I^-\cdot U$ and $I^-\cdot U\cdot H_2O$ clusters, we previously observed that the addition of water also caused an increase of approximately 0.2 – 0.3 eV eBE in the TNI binding energies.[32] The width of the VB anion photoelectron spectrum is commensurate with the VB anion measured in our past work in this photoexcitation regime as well as our near-VDE photoexcitation studies.[21-23, 32] This breadth arises due to the geometric distortion of the VB anion in the ring puckering coordinate relative to the neutral;[55, 56] thus, the presence of water does not significantly affect the uracil ring puckering as reflected by the VB anion spectral width.

In the present study, the VB anion is found to appear within the cross-correlation of the pump and probe laser pulses and decay bi-exponentially, as is the case for $I^-\cdot U$ photoexcited in this excitation energy regime. The fast decay of the $I^-\cdot U\cdot H_2O$ VB anion is similar to that of the $I\cdot U^-$ VB anion formed at 4.79 eV pump energy (Table I), while the long decay is an order of magnitude longer in the water-associated complex. This long-lived VB anion stabilization induced by the addition of water is commensurate with the dynamics that were previously observed in near-VDE photoexcited $I^-\cdot U\cdot H_2O$ clusters, in which the VB anion long-time decay was found to be significantly longer than in $I^-\cdot U$.[32]

In our previous results for π-π* photoexcited $I^-\cdot U$ and $I^-\cdot T$ clusters, we proposed that the VB anion decays by autodetachment because the measured autodetachment signals for both

clusters were found to exhibit prompt depletion and recovery near t_0 that mirrored the appearance and fast decay of the VB anion at early times, although the $I^-\cdot U$ VB anion exhibited a somewhat longer-lived bi-exponential decay.[22, 27] Given the similarities between the $I^-\cdot U$ and $I^-\cdot U\cdot H_2O$ complexes observed here, it is likely that the bi-exponential decay mechanism for the $I^-\cdot U\cdot H_2O$ VB anion in the present study is by autodetachment as well. Previously, we have attributed the bi-exponential nature of the VB anion decay to the loss of neutral iodine from the cluster, causing a reduction in the internal energy and resulting in two autodetachment decay components.[24] Neutral iodine loss was implicated our past studies of near-VDE photoexcited $I^-\cdot U$, $I^-\cdot T$, and $I^-\cdot U\cdot H_2O$ complexes and is therefore expected to be a reasonable decay pathway.[23, 24, 32] In the π-π^* photoexcitation regime, the $I\cdot T^-$ VB anion exhibits mono-exponential decay dynamics, and it has been suggested that the initial autodetachment may be faster compared to iodine loss than in $I^-\cdot U$.[24] The bi-exponential $I^-\cdot U\cdot H_2O$ VB anion decay here further indicates that the bi-exponential or mono-exponential nature of the VB anion decay is sensitive to the electronic structure of the specific nucleobase species.

C. Autodetachment dynamics

This section considers the nature of the time-resolved autodetachment signals observed in our TRPES studies. Fig. 1 shows that autodetachment signal occurs in the 4.74 eV single-photon PES of $I^-\cdot U\cdot H_2O$,[32] and therefore clearly arises from a one-photon (pump-only) process. As seen in Figs. 2 and 4, the autodetachment signal exhibits considerable intensity at all times, including negative times where the probe pulse precedes the pump pulse. Therefore, the normalized, time-resolved signals in Fig. 6 show that the autodetachment intensity exhibits little to no decrease below its intensity level at negative times. At positive probe pulse arrival times, the

autodetachment signal is found to rise in intensity within 11.3 ps and then decay in approximately 285 ps. Note that our experiment does not directly measure time-resolved autodetachment dynamics since the autodetachment electron signal is generated spontaneously and not by the probe pulse. Instead, the observed time-dependent integrated intensities associated with autodetachment signal arise from probe-based interactions that affect the amount of autodetachment signal that is detected for a given probe arrival time.

Let us compare our past measurements of autodetachment signal arising from $I^-\cdot N$ complexes to the results here for π-π* photoexcited $I^-\cdot U\cdot H_2O$. Our work on both $I^-\cdot U\cdot H_2O$ and $I^-\cdot U$ clusters has measured autodetachment arising from near-VDE photoexcitation,[23, 32] as well as from photoexcitation in the region of the base-centered π-π* transition (shown for both $I^-\cdot U\cdot H_2O$ and $I^-\cdot U$ in Fig. 7c).[21, 22, 26] Each of these past studies, regardless of photoexcitation energy, has shown autodetachment that exhibits depletion at t_0 followed by recovery to or beyond its initial intensity. Near-VDE photoexcitation in both clusters yields autodetachment signal that appears to at least qualitatively mirror the respective TNI dynamics; an example for $I^-\cdot U\cdot H_2O$ near-VDE pump autodetachment signal is shown in Fig. S1. Concomitant autodetachment signal depletion and recovery at t_0 with time constants that mirror the TNI appearance and fast decay indicates that the probe pulse at early times photodetaches the nascent TNI population that would otherwise decay to produce autodetachment signal in the absence of the probe. At later times, the probe laser interacts with a decreased population of anions that have not already undergone autodetachment, so one expects less depletion of the autodetachment signal and eventually no depletion at all. Under these circumstances, the recovery of the autodetachment signal yields the lifetime of the autodetaching state.[57]

In Fig. 7c, it can be seen that π-π* photoexcitation for both $I^-\cdot U\cdot H_2O$ and $I^-\cdot U$ clusters yields an unexpected "overshoot" of the autodetachment intensity beyond the negative-time intensity in 10s of ps. The autodetachment intensity overshoot, therefore, is uniquely associated with the VB anion generated following π-π* photoexcitation. Moreover, the similar autodetachment dynamics for $I^-\cdot U$ and $I^-\cdot U\cdot H_2O$ stand in contrast to those of π-π* photoexcited $I^-\cdot T$ clusters, which do not show any autodetachment intensity overshoot,[22] suggesting that the overshoot is also nucleobase-specific and likely related to the presence of the long-lived VB state.

This overshoot may arise if the probe pulse is absorbed by the VB anion and excites the TNI to a higher-lying excited state that subsequently decays by autodetachment, as in Eq. 5:

$$\begin{aligned} I^-\cdot U(\pi^4\pi^{*0})\cdot H_2O &\xrightarrow{h\nu_{pump}} I^-\cdot U(\pi^3\pi^{*1})\cdot H_2O \rightarrow I\cdot U^-(\pi^4\pi^{*1})\cdot H_2O \\ I\cdot U^-(\pi^4\pi^{*1})\cdot H_2O &\xrightarrow{\text{Autodetachment}} I\cdot U\cdot H_2O + e^- \\ &\xrightarrow{h\nu_{probe}} \left[I\cdot U^-(\pi^4\pi^{*1})\cdot H_2O\right]^* \xrightarrow{\text{Autodetachment}} I\cdot U\cdot H_2O + e^- \end{aligned} \quad (5)$$

The autodetachment intensity overshoot is only observed in $I^-\cdot U$ and $I^-\cdot U\cdot H_2O$ clusters, which both exhibit longer-lived, bi-exponentially decaying VB anions. $I^-\cdot T$ clusters in this pump energy region, in contrast, do not exhibit autodetachment intensity overshoot, and the VB anion decays mono-exponentially in only ~500 fs.[24] As seen in Table I, the long decay lifetimes for the VB anions of $I^-\cdot U$ and $I^-\cdot U\cdot H_2O$ clusters are in agreement with the decay lifetimes of the excess autodetachment signal. Thus, we believe a mechanism as in Eq. 5 is operative here for both $I^-\cdot U$ and $I^-\cdot U\cdot H_2O$ photoexcited in this pump energy regime.

The presence of water appears to somewhat slow the rise of the autodetachment feature (Table I), and, notably, the autodetachment signal decay lifetime is an order of magnitude longer for $I^-\cdot U\cdot H_2O$ than $I^-\cdot U$. As has been observed for the $I^-\cdot U\cdot H_2O$ VB anion both in the π-π* pump energy regime as well as the near-VDE excitation regime, the interaction of water may stabilize the excited cluster to decay by autodetachment, increasing the observed lifetime. The autodetachment signal resulting from $I^-\cdot U\cdot H_2O$ also does not appear to have depletion near t_0 as was observed in both $I^-\cdot U$ and $I^-\cdot T$ clusters.[21, 22] As noted earlier, the autodetachment depletion at early probe arrival times arises due to photodetachment of the VB excited state, which would otherwise be the spontaneous source of autodetached electrons. Lack of notable depletion in the early-time autodetachment signal of $I^-\cdot U\cdot H_2O$ as compared to $I^-\cdot U$ may therefore indicate that the $I^-\cdot U\cdot H_2O$ VB anion is more strongly stabilized relative to autodetachment than $I^-\cdot U$ clusters in this photoexcitation regime. Finally, it is interesting to note that the observed autodetachment dynamics in π-π* photoexcited $I^-\cdot U\cdot H_2O$ clusters are approximately the same in both the 1.58 eV and 3.18 eV probe energy studies (Fig. S2). It is possible, given the relatively high power of the 1.58 eV probe pulses employed in the present study, that the 1.58 eV autodetachment dynamics arise from the absorption of two probe photons by the VB anion, particularly if absorption of the first photon is resonant. This would yield similar autodetachment overshoot dynamics for each probe energy. We consider this possibility in more detail in the Supplementary Material (Fig. S3).

VI. CONCLUSIONS

TRPES has been used to examine TNI formation and photodissociation in π-π* photoexcited $I^-\cdot U\cdot H_2O$ clusters. Production of I^- is measured as a major dissociation channel of

the photoexcited clusters with bi-exponential formation in 32.5 ps and 230 ps. We suggest that the unique bi-exponential rise dynamics measured in $I^-\cdot U\cdot H_2O$ clusters in this photoexcitation regime are the result of additional dissociation channels arising from the presence of water. For example, internal conversion of the π-π* excited state and subsequent cluster dissociation is expected to yield I^-, with long-time rising signal that may be produced by dissociation of π-π* photoexcited $I^-\cdot U\cdot H_2O$ to yield $I^-\cdot H_2O$ that can subsequently decay to yield iodide. We observe instantaneous formation of the VB anion of the complex, and propose that this state arises from charge transfer from iodide to fill the empty π orbital that remains on uracil after the nucleobase is photoexcited, consistent with the proposed mechanism for $I^-\cdot U$ binary clusters. The VB anion of $I^-\cdot U\cdot H_2O$ exhibits increased binding energy compared to the VB anion of $I^-\cdot U$ clusters in this photoexcitation regime. The VB anion is found to decay bi-exponentially, as in $I^-\cdot U$, but the long decay lifetime is an order of magnitude longer in $I^-\cdot U\cdot H_2O$ clusters and is expected to reflect stabilization of the VB state relative to decay by autodetachment. Autodetachment is also measured as a dissociation channel of the photoexcited $I^-\cdot U\cdot H_2O$ complexes. Overshoot of the measured autodetachment intensity beyond the negative-time autodetachment signal indicates that absorption of the probe pulse by the long-lived VB anion produces additional autodetachment.

SUPPLEMENTARY MATERIAL

See supplementary material for additional figures of the normalized integrated intensity for the autodetachment signal arising from $I^-\cdot U\cdot H_2O$ clusters at 4.38 eV pump excitation energy and 3.14 eV probe energy, a comparison of the autodetachment signal arising from $I^-\cdot U\cdot H_2O$ clusters at 4.77 eV pump excitation energy and 1.58 eV probe energy vs. 3.18 eV probe energy, a

power-dependent study of the autodetachment dynamics as a function of the 1.58 eV probe power, and a comment on uracil tautomerization.

ACKNOWLEDGEMENTS

This research was funded by the National Science Foundation under Grant No. CHE-1663832. V.S.M. gratefully acknowledges support from a National Science Foundation Graduate Research Fellowship.

References

[1] J. Kohanoff, M. McAllister, G. A. Tribello, and B. Gu, J. Phys. - Condens. Mat. **29**, 383001 (2017).

[2] B. Boudaiffa, P. Cloutier, D. Hunting, M. A. Huels, and L. Sanche, Science **287**, 1658 (2000).

[3] F. Martin, P. D. Burrow, Z. Cai, P. Cloutier, D. Hunting, and L. Sanche, Phys. Rev. Lett. **93**, 068101 (2004).

[4] E. Alizadeh, and L. Sanche, Chem. Rev. **112**, 5578 (2012).

[5] D. Voet, W. B. Gratzer, R. A. Cox, and P. Doty, Biopolymers **1**, 193 (1963).

[6] T. Gustavsson, Á. Bányász, E. Lazzarotto, D. Markovitsi, G. Scalmani, M. J. Frisch, V. Barone, and R. Improta, J. Am. Chem. Soc. **128**, 607 (2006).

[7] Y. He, C. Wu, and W. Kong, J. Phys. Chem. A **107**, 5145 (2003).

[8] Y. He, C. Wu, and W. Kong, J. Phys. Chem. A **108**, 943 (2004).

[9] R. Barrios, P. Skurski, and J. Simons, J. Phys. Chem. B **106**, 7991 (2002).

[10] G. Hanel, B. Gstir, S. Denifl, P. Scheier, M. Probst, B. Farizon, M. Farizon, E. Illenberger, and T. D. Märk, Phys. Rev. Lett. **90**, 188104 (2003).

[11] J. Berdys, I. Anusiewicz, P. Skurski, and J. Simons, J. Am. Chem. Soc. **126**, 6441 (2004).

[12] J. Berdys, P. Skurski, and J. Simons, J. Phys. Chem. B **108**, 5800 (2004).

[13] S. Ptasińska, S. Denifl, S. Gohlke, P. Scheier, E. Illenberger, and T. D. Märk, Angew. Chem. Int. Ed. **45**, 1893 (2006).

[14] J. Simons, Accounts Chem. Res. **39**, 772 (2006).

[15] H.-Y. Chen, P.-Y. Yang, H.-F. Chen, C.-L. Kao, and L.-W. Liao, J. Phys. Chem. B **118**, 11137 (2014).

[16] M. A. Fennimore, and S. Matsika, J. Phys. Chem. A **122**, 4048 (2018).

[17] J. H. Hendricks, S. A. Lyapustina, H. L. de Clercq, and K. H. Bowen, J. Chem. Phys. **108**, 8 (1998).

[18] J. Schiedt, R. Weinkauf, D. M. Neumark, and E. W. Schlag, Chem. Phys. **239**, 511 (1998).

[19] J. Zhao, M. Wang, A. Fu, H. Yang, and Y. Bu, ChemPhysChem **16**, 2348 (2015).

[20] A. Stolow, A. E. Bragg, and D. M. Neumark, Chem. Rev. **104**, 1719 (2004).

[21] M. A. Yandell, S. B. King, and D. M. Neumark, J. Am. Chem. Soc. **135**, 2128 (2013).

[22] S. B. King, M. A. Yandell, and D. M. Neumark, Faraday Discuss. **163**, 59 (2013).

[23] S. B. King, M. A. Yandell, A. B. Stephansen, and D. M. Neumark, J. Chem. Phys. **141**, 224310 (2014).

[24] S. B. King, A. B. Stephansen, Y. Yokoi, M. A. Yandell, A. Kunin, T. Takayanagi, and D. M. Neumark, J. Chem. Phys. **143**, 024312 (2015).

[25] A. B. Stephansen, S. B. King, Y. Yokoi, Y. Minoshima, W.-L. Li, A. Kunin, T. Takayanagi, and D. M. Neumark, J. Chem. Phys. **143**, 104308 (2015).

[26] W.-L. Li, A. Kunin, E. Matthews, N. Yoshikawa, C. E. H. Dessent, and D. M. Neumark, J. Chem. Phys. **145**, 044319 (2016).

[27] A. Kunin, and D. M. Neumark, Phys. Chem. Chem. Phys. **21**, 7239 (2019).

[28] M. A. Yandell, S. B. King, and D. M. Neumark, J. Chem. Phys. **140**, 184317 (2014).

[29] A. Kunin, W.-L. Li, and D. M. Neumark, Phys. Chem. Chem. Phys. **18**, 33226 (2016).

[30] E. Matthews, R. Cercola, G. Mensa-Bonsu, D. M. Neumark, and C. E. H. Dessent, J. Chem. Phys. **148**, 084304 (2018).

[31] R. Cercola, E. Matthews, and C. E. H. Dessent, Mol. Phys., 1 (2019).

[32] A. Kunin, W.-L. Li, and D. M. Neumark, J. Chem. Phys. **149**, 084301 (2018).

[33] I. Kulakowska, M. Geller, B. Lesyng, and K. L. Wierzchowski, Biochim. Biophys. Acta, Nucleic Acids Protein Synth. **361**, 119 (1974).

[34] C. Desfrançois, H. Abdoul-Carime, and J.-P. Schermann, Int. J. Mod. Phys. B **10**, 1339 (1996).

[35] J. H. Hendricks, S. A. Lyapustina, H. L. de Clercq, J. T. Snodgrass, and K. H. Bowen, J. Chem. Phys. **104**, 7788 (1996).

[36] S. Carles, F. Lecomte, J. P. Schermann, and C. Desfrançois, J. Phys. Chem. A **104**, 10662 (2000).

[37] M. Hanus, M. Kabelac, J. Rejnek, F. Ryjacek, and P. Hobza, J. Phys. Chem. B **108**, 2087 (2004).

[38] R. A. Bachorz, W. Klopper, M. Gutowski, X. Li, and K. H. Bowen, J. Chem. Phys. **129**, 054309 (2008).

[39] J. Simons, J. Am. Chem. Soc. **103**, 3971 (1981).

[40] P. K. Acharya, R. A. Kendall, and J. Simons, J. Am. Chem. Soc. **106**, 3402 (1984).

[41] F. Mbaiwa, N. Holtgrewe, D. B. Dao, J. Lasinski, and R. Mabbs, J. Phys. Chem. A **118**, 7249 (2014).

[42] B. Baguenard, J. C. Pinaré, F. Lépine, C. Bordas, and M. Broyer, Chem. Phys. Lett. **352**, 147 (2002).

[43] C. Desfrancois, H. AbdoulCarime, and J. P. Schermann, J. Chem. Phys. **104**, 7792 (1996).

[44] O. Dolgounitcheva, V. G. Zakrzewski, and J. V. Ortiz, Chem. Phys. Lett. **307**, 220 (1999).

[45] O. Dolgounitcheva, V. G. Zakrzewski, and J. V. Ortiz, J. Phys. Chem. A **105**, 8782 (2001).

[46] R. A. Bachorz, W. Klopper, and M. Gutowski, J. Chem. Phys. **126**, 085101 (2007).

[47] R. J. Peláez, C. Blondel, C. Delsart, and C. Drag, J. Phys. B-At. Mol. Opt. **42**, 125001 (2009).

[48] A. V. Davis, R. Wester, A. E. Bragg, and D. M. Neumark, J. Chem. Phys. **118**, 999 (2003).

[49] A. E. Bragg, J. R. R. Verlet, A. Kammrath, O. Cheshnovsky, and D. M. Neumark, J. Am. Chem. Soc. **127**, 15283 (2005).

[50] W. C. Wiley, and I. H. McLaren, Rev. Sci. Instrum. **26**, 1150 (1955).

[51] A. Eppink, and D. H. Parker, Rev. Sci. Instrum. **68**, 3477 (1997).

[52] V. Dribinski, A. Ossadtchi, V. Mandelshtam, and H. Reisler, Rev. Sci. Instrum. **73**, 2634 (2002).

[53] G. Markovich, R. Giniger, M. Levin, and O. Cheshnovsky, J. Chem. Phys. **95**, 9416 (1991).

[54] G. Markovich, S. Pollack, R. Giniger, and O. Cheshnovsky, J. Chem. Phys. **101**, 9344 (1994).

[55] T. Sommerfeld, J. Phys. Chem. A **108**, 9150 (2004).

[56] T. Takayanagi, T. Asakura, and H. Motegi, J. Phys. Chem. A **113**, 4795 (2009).

[57] R. M. Young, M. A. Yandell, and D. M. Neumark, J. Chem. Phys. **134**, 124311 (2011).

Table I. Lifetimes for the VB anion, autodetachment feature, and I^- feature for 4.77 eV pump $I^-\cdot U\cdot H_2O$ and comparison to previous $I^-\cdot U$ studies. The $I^-\cdot U$ data for the VB anion and autodetachment dynamics are from Ref. [21], and for the I^- feature the data is from Ref. [26].

VB anion			
Cluster	$h\nu_{pump}$	$\tau_{decay,\ 1}$	$\tau_{decay,\ 2}$
$I^-\cdot U\cdot H_2O$	4.77 eV	540 ± 240 fs	220 ± 70 ps
$I^-\cdot U$	4.79 eV	390 ± 80 fs	37 ± 20 ps
Autodetachment			
Cluster	$h\nu_{pump}$	τ_{rise}	τ_{decay}
$I^-\cdot U\cdot H_2O$	4.77 eV	11.3 ± 2.2 ps	285 ± 70 ps
$I^-\cdot U$	4.79 eV	~5 ps	~50 ps
I^-			
Cluster	$h\nu_{pump}$	$\tau_{rise,\ 1}$	$\tau_{rise,\ 2}$
$I^-\cdot U\cdot H_2O$	4.77 eV	32.5 ± 2.6 ps	230 ± 20 ps
$I^-\cdot U$	4.72 eV	36 ± 3 ps	

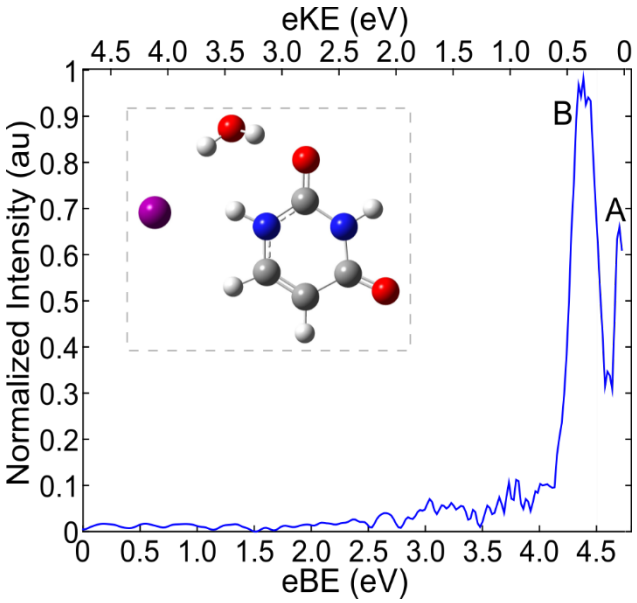

Figure 1. Single-photon photoelectron spectrum of $I^-\cdot U\cdot H_2O$ at 4.74 eV and calculated ground state $I^-\cdot U\cdot H_2O$ structure (inset). The spectrum and structure are adapted from Kunin et al., J. Chem. Phys., 2018, **149**, 084301, with the permission of AIP Publishing.

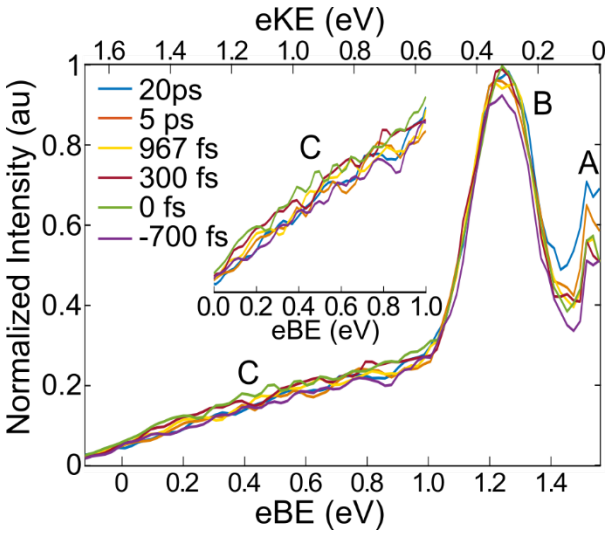

Figure 2. Photoelectron spectra of $I^-\cdot U\cdot H_2O$ at 4.77 eV pump excitation energy and 1.58 eV probe energy at selected delay times.

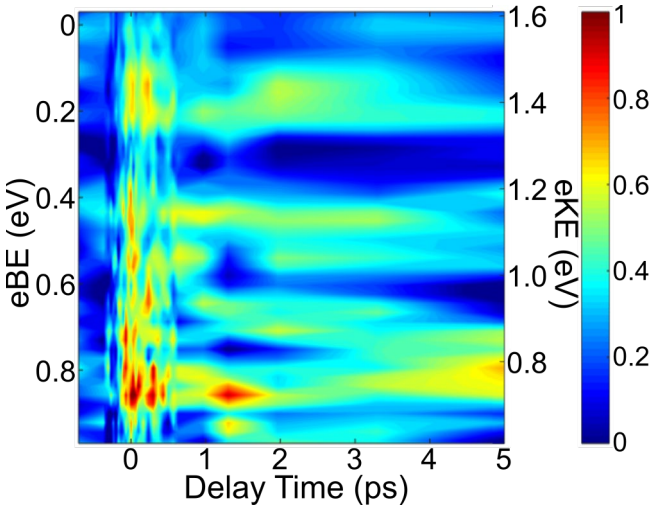

Figure 3. Representative background-subtracted time-resolved photoelectron spectra for feature C at short pump-probe delays for $I^{-}\cdot U\cdot H_2O$ at 4.77 eV pump excitation energy and 1.58 eV probe energy.

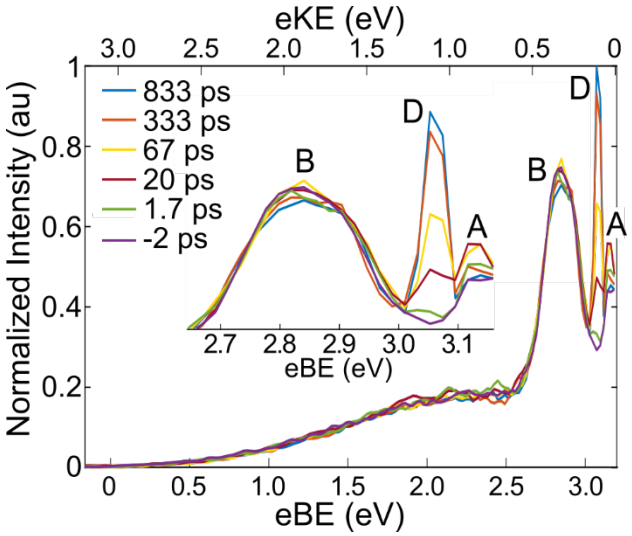

Figure 4. Photoelectron spectra of $I^{-}\cdot U\cdot H_2O$ at 4.77 eV pump excitation energy and 3.18 eV probe energy at selected delay times.

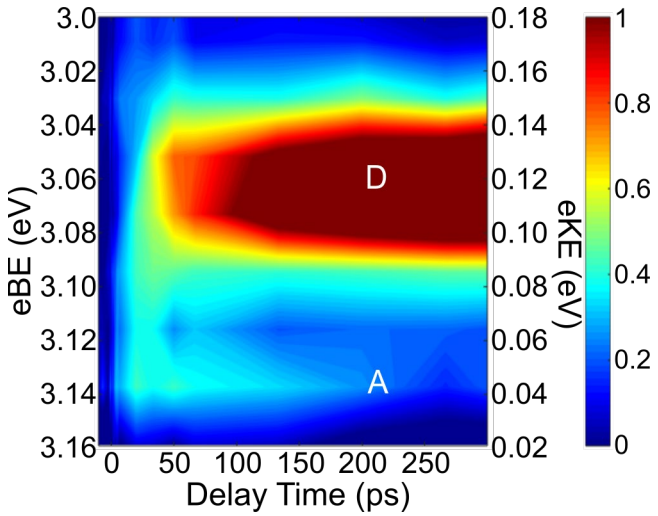

Figure 5. Representative background-subtracted time-resolved photoelectron spectra for features A (near maximum eBE, eKE ~ 0 – 0.07 eV), and D (eBE = 3.06 eV) for $I^-\cdot U\cdot H_2O$ at 4.77 eV pump excitation energy and 3.18 eV probe energy.

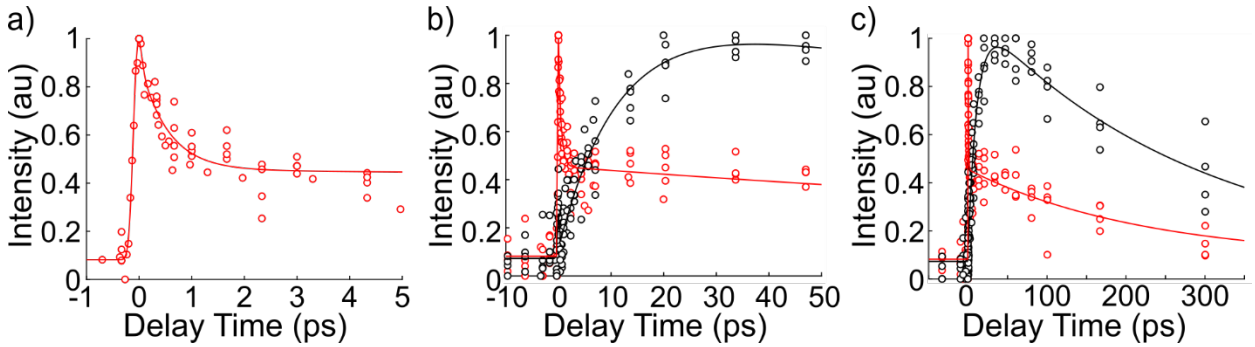

Figure 6. Concatenated normalized integrated intensities for features A (black, autodetachment) and C (red, VB anion) at a) early time delays, b) 10s of ps, and c) long time delays from excitation at 4.77 eV and probed with 1.58 eV. Feature A rises in 11.3 ± 2.2 ps and decays in 285 ± 70 ps. The rise time for feature C is cross-correlation limited and the decay is 540 ± 240 fs and 220 ± 70 ps.

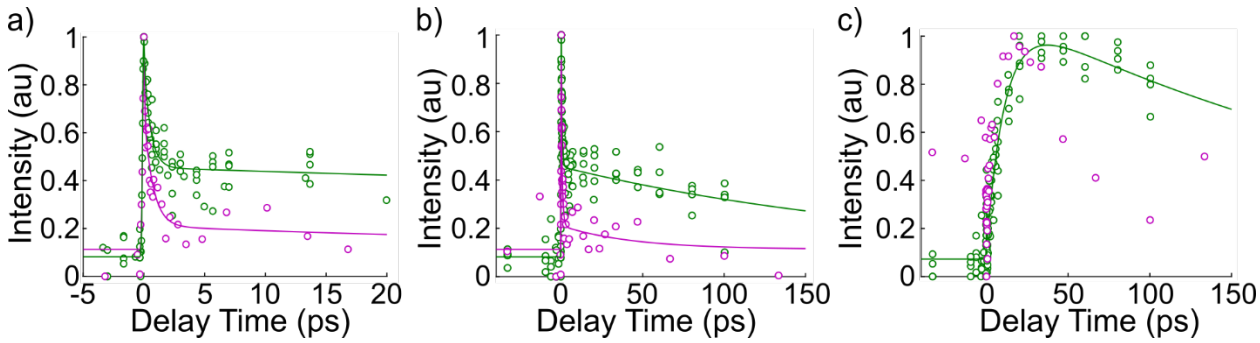

Figure 7. Comparison of concatenated normalized integrated intensities for a) the VB anion at early times and b) long times and c) autodetachment dynamics for $I^-\cdot U\cdot H_2O$ (green) at 4.77 eV pump excitation energy and 1.58 eV probe energy and $I^-\cdot U$ (purple) at 4.79 eV pump excitation energy and 1.57 eV probe energy.

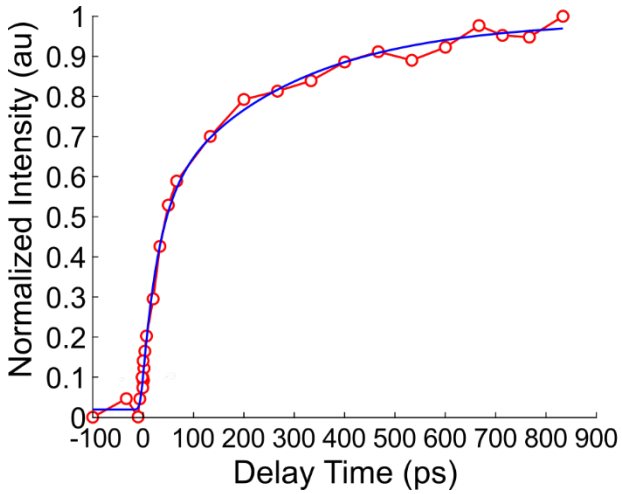

Figure 8. Normalized integrated intensity for feature D at 4.77 eV pump excitation energy and 3.18 eV probe energy. Feature D rises bi-exponentially with time constants of 32.5 ± 2.6 ps and 226 ± 20 ps.